



Article

Experimental investigation of cycling characteristics of anatase TiO₂ nanotubes as negative electrode of lithium-ion batteries

Simul Das¹, Md. Arafat Rahman*¹, Md. Saiful Islam², Konok Chandra Bhowmik¹¹Department of Mechanical Engineering, Chittagong University of Engineering & Technology, Chittagong-4349, Bangladesh²Department of Nanomaterials and Ceramic Engineering, Bangladesh University of Engineering and Technology, Dhaka-1000, Bangladesh

ARTICLE INFO

Article history:

Received 28 September 2024

Received in revised form

01 November 2024

Accepted 14 November 2024

Keywords:

Anatase, TiO₂, Nanotube, Anode, Lithium-ion Battery

*Corresponding author

Email address:

arafat@cuet.ac.bd

DOI: 10.55670/fpll.fuen.3.4.1

ABSTRACT

Anatase TiO₂ Nanotubes (NT-TiO₂) is synthesized via electrochemical anodization of 99.9% pure titanium foils in a fluorine containing Ethylene Glycol (EG) electrolyte and used as the anode of lithium-ion batteries (LIBs). In the first cycle, the charge-discharge capacities are 550 mAhg⁻¹ and 400 mAhg⁻¹, respectively, with coulombic efficiency of 75.75%. At 40th cycle, charge-discharge capacities are found to be 375 mAhg⁻¹ and 325 mAhg⁻¹, respectively, with improved coulombic efficiency of 86%. The superior electrochemical performances of this type of battery originated from its high specific surface area and highly nanotubes structure. These advanced features of the nanotubes provide higher contact between electrodes and electrolytes, shorten the diffusion pathways for conductive ions.

1. Introduction

Lithium-ion batteries (LIBs) have emerged as a game-changing technology in the search for effective and sustainable energy storage solutions. They have revolutionized modern portable electronics and made it possible to electrify several industries, including grid energy storage and transportation [1]. LIBs have replaced traditional energy storage systems because of their superior features, including high energy density, extended cycle life, and lightweight design for greater portability. The field of LIBs has observed continuous advancements in response to the increasing demand for energy storage systems with better performance metrics, such as higher energy density, quicker charging times, improved safety, and longer lifespans. In addition, the field of batteries for energy has witnessed considerable interest in the domain of nanofabrication. A multitude of materials for anodes have been identified, therefore instigating continuous investigations aimed at ascertaining feasible alternatives. The utilization of TiO₂, a transition oxide of metals, as a material for anodes in batteries powered by lithium ions offers a potentially advantageous substitute for traditional graphite [2, 3]. The investigation

into the use of TiO₂ substances for anode applications may be traced back to the identification of the capability of lithium titanites to conduct lithium insertion activities. Recently, there has been a growing interest in exploring the potential Li-insertion properties of titanite spinels. This has led to a heightened focus on investigating different nanostructures of TiO₂ polymorphs, specifically for their applicability in Li-ion battery systems. Rutile, which is considered the most thermally stable polymorph of TiO₂, demonstrates a restricted ability to incorporate lithium ions, with a capacity of fewer than 0.1 lithium ions per unit of TiO₂ at room temperature [4]. Li-reactivity was higher at a temperature of 120°C when using a polymeric electrolyte instead of a liquid electrolyte. In these conditions, the first discharge reversible capacities were reported to be 0.5 Li [2] and 1 Li [5] per formula unit of TiO₂. It is noted that the diffusion of Li in rutile exhibits a significant degree of anisotropy, characterized by rapid diffusion primarily along the channels aligned with the c-axis [6-10]. The utilization of a well-aligned and self-organized TiO₂ nanostructure array presents a promising opportunity for its application as a potential anode material in LIBs. It is noted that difficulties observed in the utilization

of traditional graphite as a material for anodes in LIBs, such as the formation of SEI layers, dendritic effects, exfoliation over cycling, toxicity, and structural collapse [11, 12]. The primary impetus behind this research stems from the need to address these limitations and explore alternative anode materials that possess desirable properties, with the goal of proposing a potential replacement for conventional graphite anodes. Anatase TiO₂ has a theoretical capacity of TiO₂ is slightly lower (330mAhg⁻¹) compared to graphite's capacity of 372mAhg⁻¹; the focus of research has primarily been on the structural stability of TiO₂. This work highlights the usage of anatase TiO₂ nanotubes as the anode of LIBs. These nanotubes are created by anodizing pure Ti foils in a neutral fluoride solution, followed by calcination. Nanotube anatase structures with a significantly high specific area were created by carefully regulating the anodization and calcination processes. The primary cause of an interfacial process whereby lithium was stored on the surface of anatase particles was this sizable, exposed electrode area. The high specific surface area of anatase TiO₂ nanotubes electrodes exhibits the first cycle charge-discharge capacities are 550 mAhg⁻¹ and 400 mAhg⁻¹, respectively, with columbic efficiency of 75.75%. However, this electrode exhibited improved electrochemical performances of 375 mAhg⁻¹ and 325 mAhg⁻¹, respectively, with improved columbic efficiency of 86% after 40th charge-discharge cycle.

2. Experimental

2.1 Fabrication of anatase TiO₂ nanotubes

Using a Pt plate as the cathode, 99.9% pure Ti foil was oxidized to create TiO₂ nanotubes by the anodization process. The samples, particularly the Ti foils, were cleaned for 30 minutes using distilled water and detergent water prior to anodization. After that, the samples were cleaned for ten minutes in a pure ethanol solution. Following that, a final 20-minute acetone immersion rinse was performed. After that, the samples were dried for 24 hours at 105 °C. Two groups of all the Ti samples that needed to be anodized were created. One set of samples was cleaned with distilled water after being scraped with 0-grade emery paper. Both sets of Ti foils underwent anodization in a water-based solution that contained 0.5 wt.% NH₄F + 1M (NH₄)₂SO₄ + 10% of ethylene glycol (EG). Anodization took place in a 100 ml solution, indicating that the electrolyte comprised 100 ml of distilled water, 0.5g NH₄F (supplied by SUEN STUDIO, China), and 13.2g 1M (NH₄)₂SO₄ (supplied by SUEN STUDIO, China). The anode and cathode were connected to the positive and negative terminals of the DC power supply, respectively. The DC power supply's positive and negative terminals were linked to the anode and cathode, respectively. A DC power supply (DAZHENG brand, model PS-3050, China) provided a steady 32 V DC voltage for one hour and two hours, respectively, while maintaining a zero-current flow.

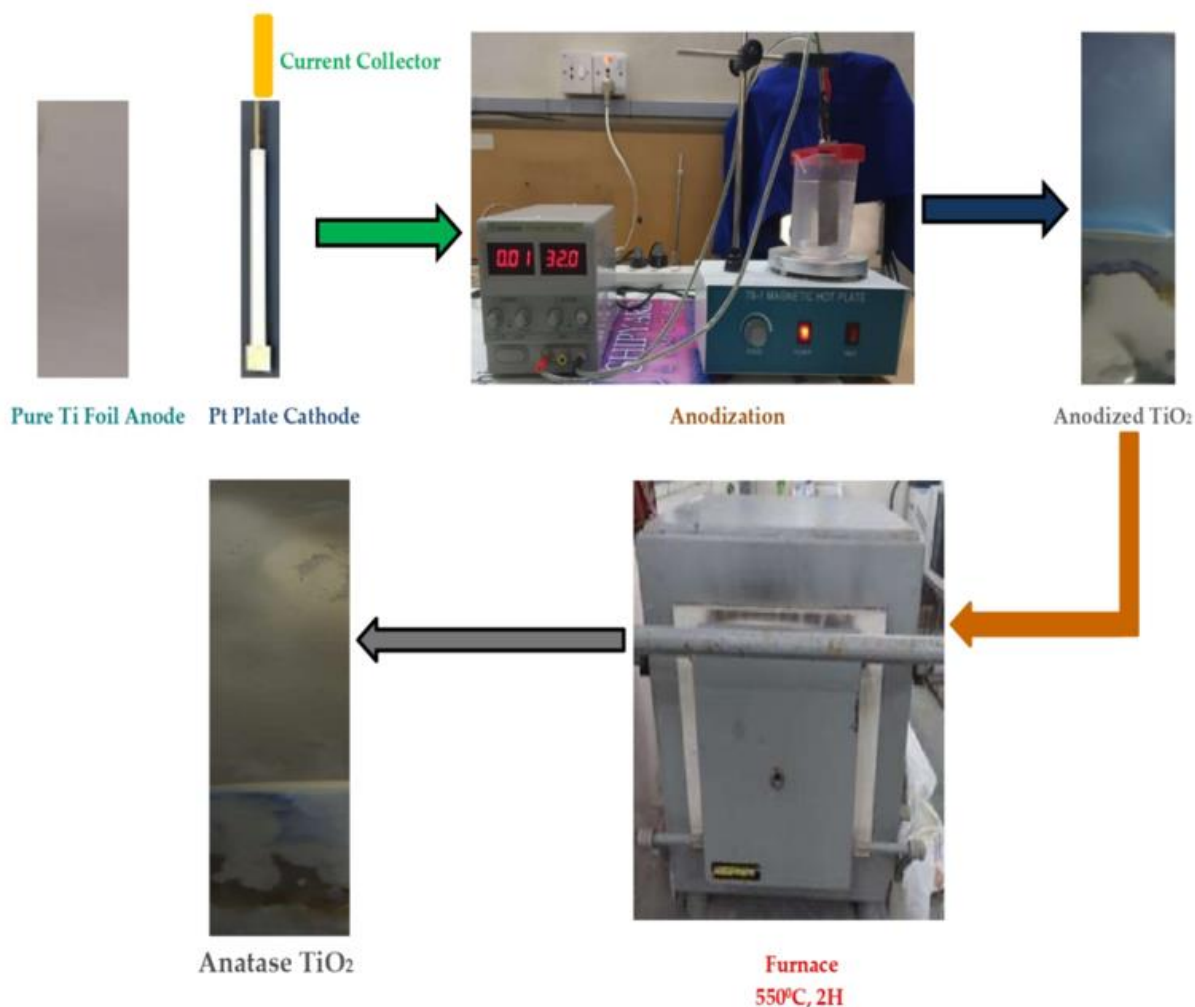


Figure 1. Visual representation of fabrication steps of anatase TiO₂ nanotubes

A magnetic stirrer hotplate ('78-1 Magnetic Stirrer Hotplate,' Yaeccc brand, China) at an average speed of 400 rpm during the anodization process verified that the solutes in solution were mixed uniformly and that the ions were moving properly. Following anodization, the anodized section of Ti foils changed from having a grey appearance to a bluish one. After being cleansed with distilled water, all samples were put in a furnace and calcined for two hours at 550°C. The full process is depicted in Figure 1.

2.2 Characterization

The NT-TiO₂ samples were analyzed using X-Ray Powder Diffraction (XRD) to obtain crystallographic information. To account for various scattering and random orientations, scans were conducted at different 2θ angles. Our analysis covered a 2θ range from 10° to 90° with a step size of 0.05°, utilizing Cu Kα radiation (Empyrean, Panalytical-Netherlands) with a wavelength of $\lambda = 1.5406\text{Å}$. The morphological and compositional characterization of anatase TiO₂ nanotubes was carried out using scanning electron microscopy and energy dispersive X-ray spectroscopy (SEM-EDX). For our experiment, SEM-EDX images were captured with a JSM 7600F from JEOL (Japan) at 5.0 KV and various magnifications.

2.3 Electrochemical performance test

Coin cell battery case sets CR2032 (provided by Lith Co. China) were utilized for assembly purposes. Anode samples measuring 18 mm in diameter and 0.1 mm in thickness (approximately 2 cm²) of NT-TiO₂, along with LiCoO₂ coated aluminum sheet cathodes and a 20 mm battery grade PVC separator, fit perfectly into the cases. Both sides of the separator were saturated with a few drops of 1M LiPF₆ (from Ximen Tmax Battery Equipment Ltd., China) electrolyte, which was mixed in ethylene carbonate (EC) and diethylene carbonate (DEC) at a ratio of 3:7. Finally, crimping was performed at a pressure of about 100 psi using a battery crimping machine (Metrology Lab, CUET).

3. Results & discussion

3.1 XRD analysis

As illustrated in Figure 2, the X-ray diffraction (XRD) technique is used to analyze the phase purity and crystallinity of Ti and anatase TiO₂ nanotubes. TiO₂ has a tetragonal body-centered crystal structure from space group I41/amd, and the lattice parameters for samples and Ti foil are $a = 3.79\text{Å}$, $c = 9.51\text{Å}$. The anatase phase of TiO₂ is confirmed by these data. Furthermore, the values match standard data (JCPDS Card no. 21-1272) exactly. At diffraction 2θ angles of 39.910 (101 plane), 52.770 (012 plane), and 70.4190 (013 plane), however, more noticeable anatase peaks are seen. The lack of any impurity phases within the detection range of the diffractometer indicates the purity of Ti. It is observed that no additional diffraction peaks related to the oxide phase were observed. Utilizing Scherrer's formula, $D = 0.9\lambda / B \cos(\theta)$, with λ representing the X-ray wavelength in nanometers, B representing the full width at half maximum (FWHM) of peaks at 2θ, and θ representing the angle between the incident and diffracted beams in degrees, these diffraction data are entered. Table 1 displays the crystal sizes of Ti foil and the synthesized anatase NT-TiO₂ at various 2θ angles.

3.2 SEM & EDX analysis

The plan-view SEM images and EDX spectra of anatase NT-TiO₂ is shown in Figure 3. Non-uniform anatase NT-TiO₂ arrays is grown by anodization, which is observed clearly underneath the Ti substrates as shown in Figure 3(a). The nanotubes are compact in this area. For the elemental characterization of the obtained nanotube layers, energy dispersive X-ray analysis is conducted. The EDX spectrum indicates the presence of the TiKα peak at 4.508 keV and O peaks at 0.525 keV as well as C peak at 0.277 keV in the anodized sample as shown in Figure 3(b). The obtained mass percentages of Ti and O is observed to be 55.30% and 42.44%, respectively, and the atom percentage of Ti, O, and C is 28.93%, 66.81%, and 4.26%, respectively. It is noted that peak of carbon is found at 0.277 keV with the percentage of C is 2.04%.

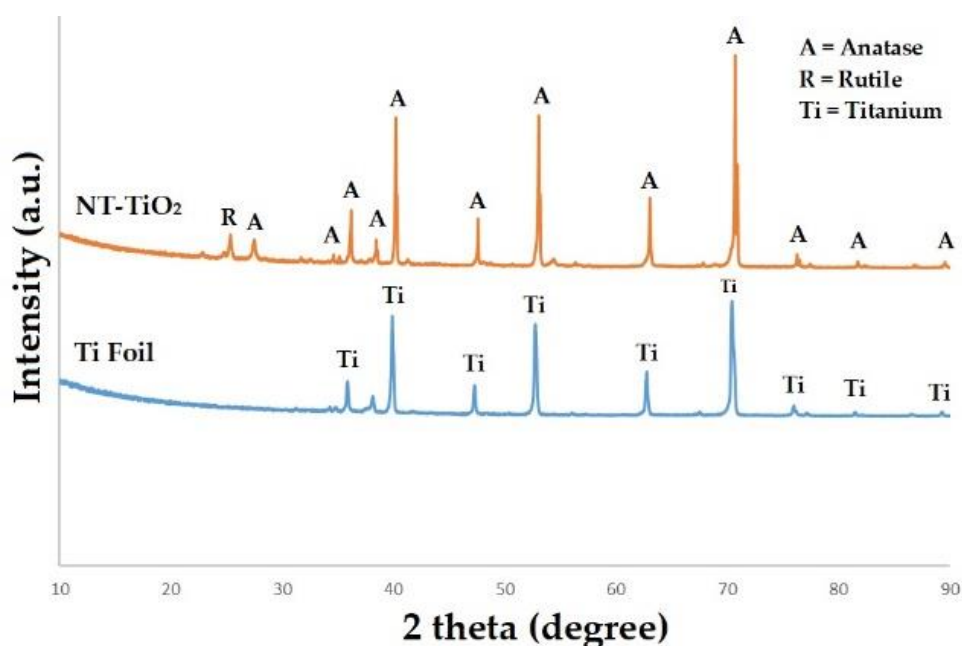


Figure 2. XRD patterns of different anatase NT-TiO₂ along with pure Ti

Table 1. Crystal Sizes Ti foil and as synthesized anatase NT-TiO₂

Sample No.	Crystallographic Data for Pure Ti											Average Crystal Size (nm)
	2θ	35.90	38.14	39.92	47.30	52.77	62.78	70.42	-	-	-	
a	B	0.22	0.32	0.23	0.20	0.26	0.22	0.33	-	-	-	38.27
	D	40.42	28.01	38.76	46.31	36.18	46.02	32.16	-	-	-	
	Crystallographic Data of NT-TiO ₂											
b	2θ	22.87	25.37	27.51	36.21	38.47	40.23	47.61	53.06	63.07	70.71	65.66
	B	2.07	0.36	0.44	0.16	0.16	0.10	0.10	0.09	0.13	0.09	
	D	4.21	24.39	20.09	56.26	58.35	89.19	92.14	111.45	80.33	120.18	

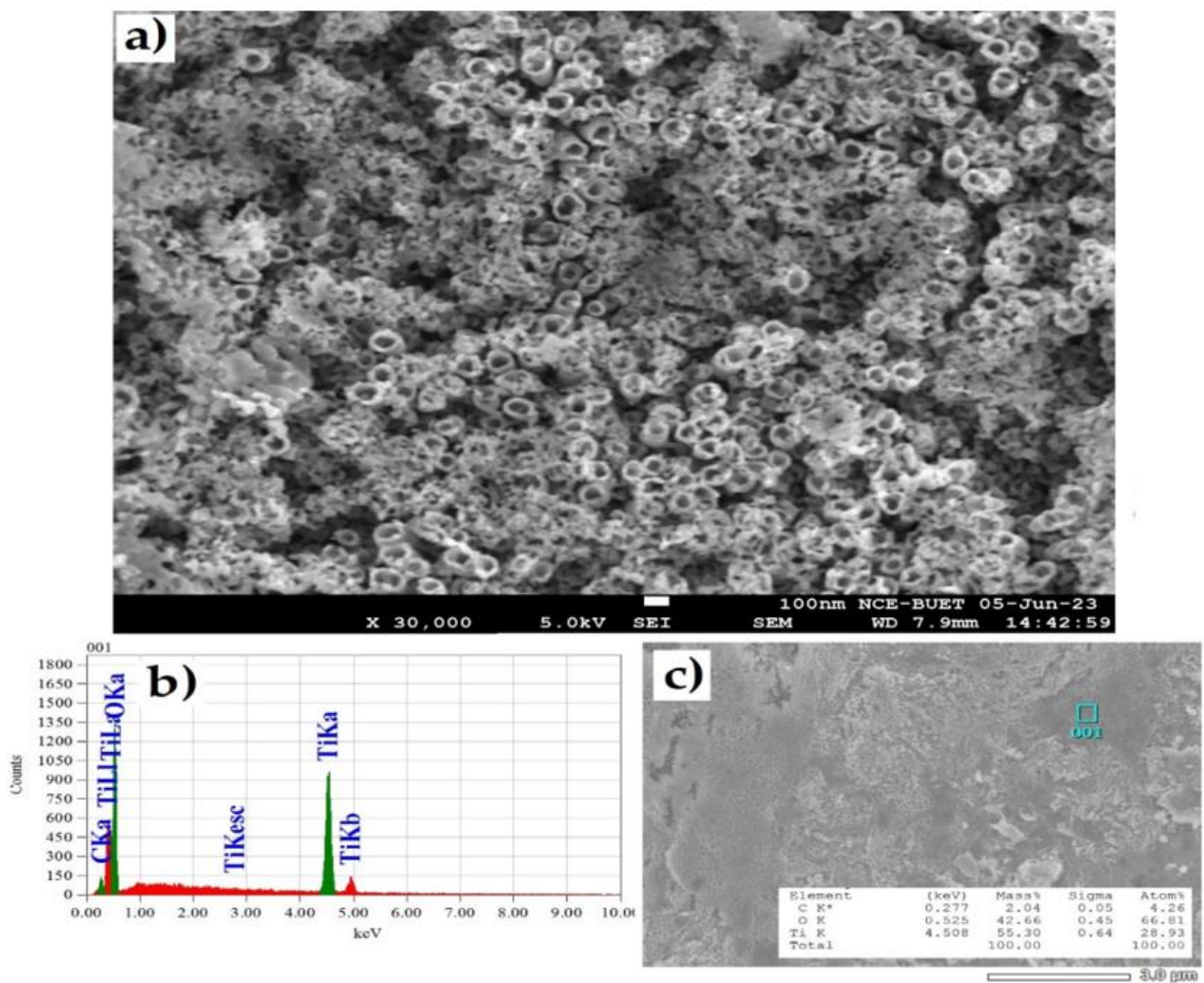


Figure 3. High magnification SEM image and EDX spectra of anatase NT-TiO₂

3.3 Electrochemical performance of anatase NT-TiO₂ as anode of LIBs

The galvanostatic charge-discharge cycle is carried out to measure the electrochemical performance of the as-prepared anatase NT-TiO₂ anode. Figures 4(a & b) show the changes in current and voltage with respect to charge-discharge time. The cut-off voltage ranges are 4V-3.8V. It is noted that the voltages remain 2.5V at the beginning of the cycling, as shown in Figure 4(a). However, the voltage increases as the cycling moves forward, and after the 20th cycle, the voltage decreases. In contrast, the voltage and current both increase at the end of the 40th cycle of the charge-discharge process, where the voltage is found to be 4.2V, as shown in Figure 4(b). Figure 4(c) shows a variation in the rate of change in charge with a change in voltage (dQ/dV) till 40 charge-discharge cycles for incremental capacity analysis, which identifies and quantifies changes in the electrochemical properties of the cell based on voltage measurements under constant current charge or discharge. It is observed that the phase transitions in the active electrode material anatase NT-TiO₂ caused by the intercalation and deintercalation of lithium at about 2.5V correlate with the incremental capacity peaks. It is worth mentioning that dQ/dV analysis indicates the electrochemical performances of cell degradation over charge-discharge cycling, as shown in Figure 4(c), due to an increase in internal resistance [13]. Figure 5 shows the charge-discharge capacity and Columbic efficiency of LIB till 40 cycles. First cycle charge-discharge capacities are 550 mAhg⁻¹ and 400 mAhg⁻¹, respectively, with columbic efficiency of 75.75%, as shown in Figure 5(a). Higher initial capacities are ascribed to gel-like SEI layer formation by electrolyte decomposition [14]. In addition, the low columbic efficiency is attributed to unstable SEI formation, low reversible capacity, and electrolyte decomposition.

However, in the subsequent 2nd cycle, the charge-discharge capacity comparably reduced to 500 mAhg⁻¹ and 360 mAhg⁻¹, respectively, due to the amorphous Li₂O formation, which required a huge amount of lithium and caused the loss of lithium [2]. The increased columbic efficiency of 75.4% in the 2nd cycle is attributed to stable SEI layer formation. It is noted that the cell shows instability with fluctuating columbic efficiency, which is attributed to the larger volume expansion and pulverization effect of the anode. In addition, at the 27th cycle, the columbic efficiency is as high as 120%, as shown in Figure 5(b). This phenomenon is typical for transition metal oxides due to the pseudo capacitance [15-17]. At the 40th cycle, charge-discharge capacities are found to be 375 mAhg⁻¹ and 325 mAhg⁻¹, respectively, and the columbic efficiency is observed to be 80%, which is comparable to the theoretical capacity of TiO₂ 334 mAhg⁻¹. Table 2 shows the comparison of charge and discharge capacities of this present work and previous work. It is noted that the charge-discharge capacities of this present work at 1st is observed to be 550 mAhg⁻¹ and 400 mAhg⁻¹, respectively, which is higher compared to 290 mAhg⁻¹ and 239 mAhg⁻¹, respectively. However, the observed Columbic efficiency is slightly lower, 75%, compared to the previous work of 82%. This deficiency could be ascribed to the impurities in the electrolytes, and/or our cell is assembled in ambient without using a glovebox [18]. However, the electrochemical performances and Columbic efficiency increased after the 40th charge-discharge cycle compared to the previous work. Here, we are anticipating that the Columbic efficiency will be improved over a large number of cycling of our synthesized material since Columbic efficiency rises and irreversible capacity falls after the irreversible Li insertion sites are filled and trace water has been used up in the first cycles [14].

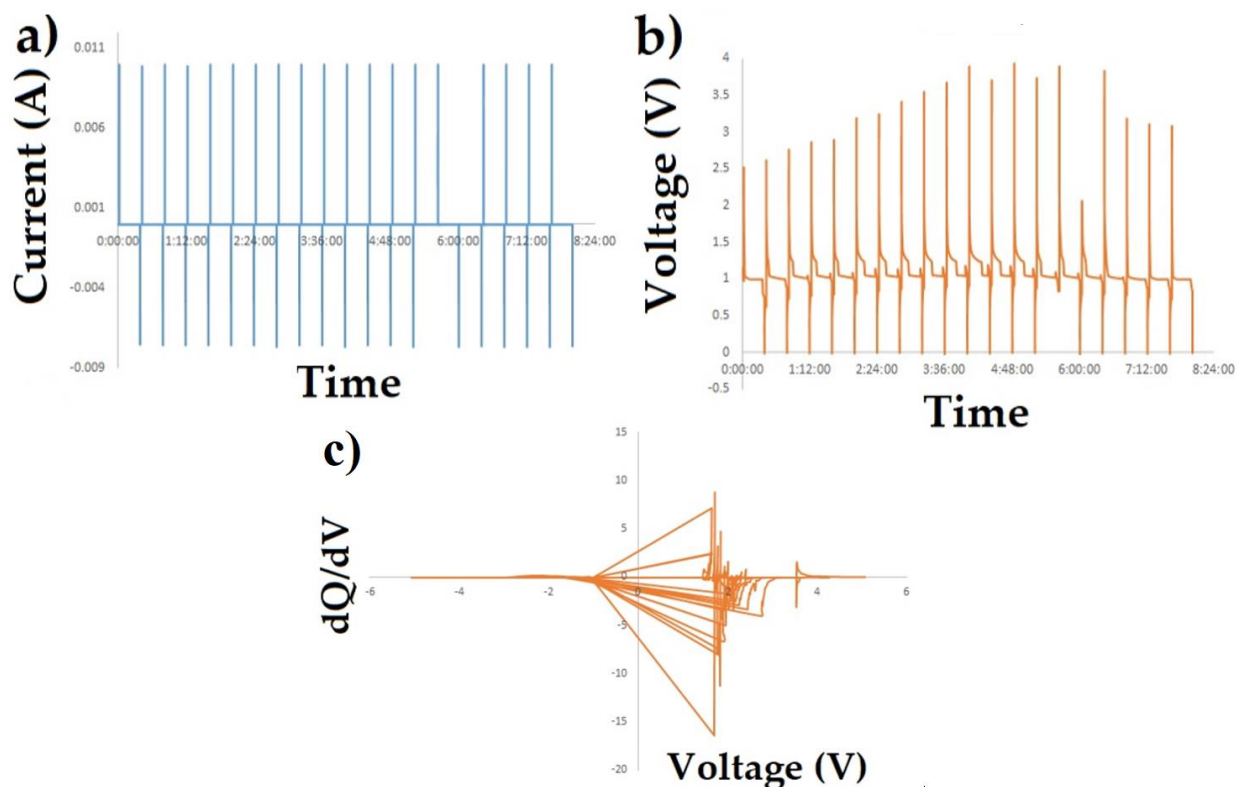


Figure 4. Change of (a) Current (b) Voltage with respect to time from 1-20 Charge-Discharge cycles, c) Change of dQ/dV with respect to voltage from 1-40 cycles

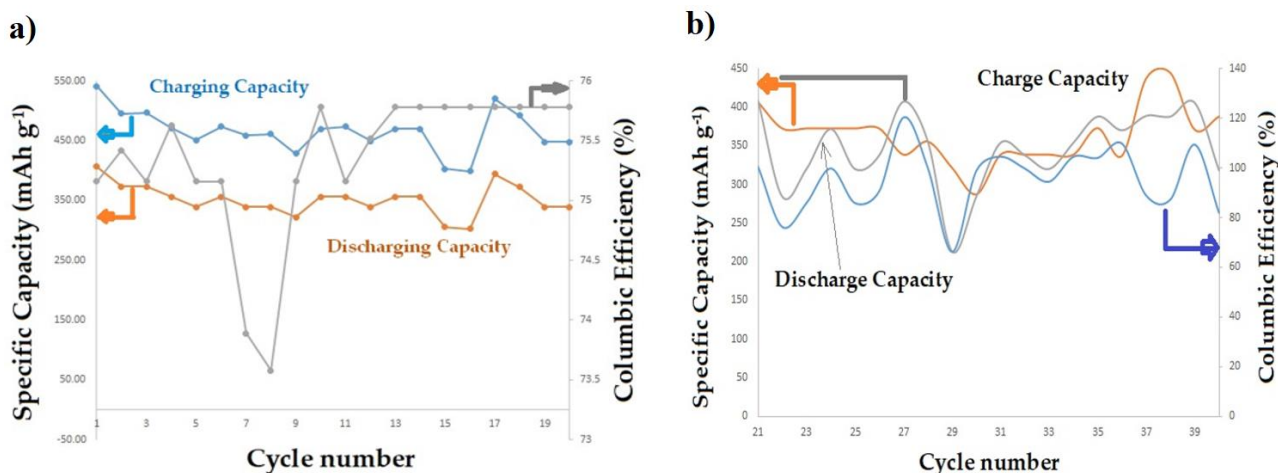


Figure 5. Change of Specific capacity and columbic efficiency during (a) 1-20 and (b) 21-40 charge-discharge cycles at 1C current rating

Table 2. Comparison of our work with previous work

Compare	Cycle No.	Unit	Our Work	Previous Work	Reference
Charge Capacity	1st	mAhg ⁻¹	550	290	[19, 20]
Discharge Capacity		mAhg ⁻¹	400	239	
Columbic Efficiency		%	75	82	
Charge Capacity	40 th /Last	mAhg ⁻¹	375	238	
Discharge Capacity		mAhg ⁻¹	325	198	
Columbic Efficiency		%	86	83	

4. Conclusion

Anatase TiO₂ nanotube has been considered as one of the most attractive anode materials for lithium-ion batteries (LIBs) due to comparable energy density and life cycle compared to graphite. The nanotube features of nanostructure provide higher contact between binder-less electrode TiO₂ and electrolytes, shorten the diffusion pathways for conductive ions and electrons that ensure faster kinetics. The work represents a facile fabrication of anatase NT-TiO₂ via electrochemical anodization of Ti foils. Anatase NT-TiO₂ is used as anode LIBs. Nanotubes provide a high surface area that allows for a higher electrode/electrolyte interface. Hence, lithium storage capacity is greatly enhanced compared to bulk amorphous TiO₂. The cut-off voltage ranges are 4V-3.8V. It is noted that at the beginning of the cycling, the voltages remain at 2.5V. However, as the cycling moves forward, the voltage increases, and at the end of the 40th cycle of the charge-discharge process, the voltage is found to be 4.2V. The battery exhibits excellent 1st cycle charge-discharge capacity of 550 mAhg⁻¹ and 400 mAhg⁻¹, respectively, with 75.75% columbic efficiency. At the 27th cycle, the columbic efficiency is as high as 120%. This phenomenon is typical for transition metal oxide due to the pseudo-capacitance. At the 40th cycle, charge-discharge capacities are found to be 375 mAhg⁻¹ and 325 mAhg⁻¹, respectively, and the columbic efficiency is found to be 86%. The findings showed that anatase TiO₂ nanotubes' large surface area, short diffusion path, and quick kinetics make them promising electrode materials for LIB applications.

Acknowledgments

This work is financially supported by Chittagong University of Engineering & Technology (CUET), Bangladesh, through Research Grant no.: CUET/CHSR-43-43.8.6.

Ethical issue

The authors are aware of and comply with best practices in publication ethics, specifically concerning authorship (avoidance of guest authorship), dual submission, manipulation of figures, competing interests, and compliance with policies on research ethics. The authors adhere to publication requirements that the submitted work is original and has not been published elsewhere in any language.

Data availability statement

The manuscript contains all the data. However, more data will be available upon request from the corresponding author.

Conflict of interest

The authors declare no potential conflict of interest.

References

[1] Chy, M.N.U., et al., MXene as Promising Anode Material for High-Performance Lithium-Ion Batteries: A Comprehensive Review. 2024. 14(7): p. 616.
 [2] Rahman, M.A., et al., Improvement on electrochemical performances of nanoporous titania as anode of lithium-ion batteries through annealing of pure titanium foils. 2018. 27(1): p. 250-263.
 [3] Rahman, M.A., X. Wang, and C.J.J.o.E.C. Wen, Enhanced electrochemical performance of Li-ion batteries with

- nanoporous titania as negative electrodes. 2015. 24(2): p. 157-170.
- [4] Kavan, L., M.J.E. Graetzel, and S.-S. Letters, Facile synthesis of nanocrystalline $\text{Li}_4\text{Ti}_5\text{O}_{12}$ (Spinel) exhibiting fast Li insertion. 2001. 5(2): p. A39.
- [5] Kavan, L., D. Fattakhova, and P.J.J.o.t.E.S. Krtil, Lithium Insertion into Mesoscopic and Single-Crystal TiO_2 (Rutile) Electrodes. 1999. 146(4): p. 1375.
- [6] Zachau-Christiansen, B., et al., Lithium insertion in different TiO_2 modifications. 1988. 28: p. 1176-1182.
- [7] Macklin, W. and R.J.S.S.I. Neat, Performance of titanium dioxide-based cathodes in a lithium polymer electrolyte cell. 1992. 53: p. 694-700.
- [8] Koudriachova, M.V., N.M. Harrison, and S.W.J.S.S.I. de Leeuw, Diffusion of Li-ions in rutile. An ab initio study. 2003. 157(1-4): p. 35-38.
- [9] Johnson, O.J.P.R., One-dimensional diffusion of Li in rutile. 1964. 136(1A): p. A284.
- [10] Koudriachova, M.V., N.M. Harrison, and S.W.J.P.R.L. de Leeuw, Effect of diffusion on lithium intercalation in titanium dioxide. 2001. 86(7): p. 1275.
- [11] Ruan, C., et al., Fabrication of highly ordered TiO_2 nanotube arrays using an organic electrolyte. 2005. 109(33): p. 15754-15759.
- [12] Moradi, B. and G.G.J.J.o.A.E. Botte, Recycling of graphite anodes for the next generation of lithium ion batteries. 2016. 46: p. 123-148.
- [13] Wang, R., et al., Degradation analysis of lithium-ion batteries under ultrahigh-rate discharge profile. 2024. 376: p. 124241.
- [14] Munonde, T.S. and M.C.J.J.o.E.S. Raphulu, Review on titanium dioxide nanostructured electrode materials for high-performance lithium batteries. 2024. 78: p. 110064.
- [15] Paul, S., et al., TiO_2 as an Anode of high-performance lithium-ion batteries: A Comprehensive Review towards Practical Application. 2022. 12(12): p. 2034.
- [16] Zhang, Y., et al., Nanostructured TiO_2 -Based Anode Materials for High-Performance Rechargeable Lithium-Ion Batteries. 2016. 2(8): p. 764-775.
- [17] Paul, S., et al., Nanostructured anatase TiO_2 as anode of high-performance lithium-ion batteries. 2022. 1(4): p. 20220018.
- [18] Wang, L., S. Riedel, and Z.J.A.E.M. Zhao-Karger, Challenges and Progress in Anode-Electrolyte Interfaces for Rechargeable Divalent Metal Batteries. 2024: p. 2402157.
- [19] Xu, J., et al., Electrochemical properties of anatase TiO_2 nanotubes as an anode material for lithium-ion batteries. 2007. 52(28): p. 8044-8047.
- [20] Jiang, Y., et al., Fabrication strategies for high-rate TiO_2 nanotube anodes for Li ion energy storage. 2020. 463: p. 228205.



This article is an open-access article distributed under the terms and conditions of the Creative Commons Attribution (CC BY) license (<https://creativecommons.org/licenses/by/4.0/>).